EFFECTS OF RECTIFICATION ON SYNAPTIC EFFICACY

RONALD W. JOYNER
Department of Physiology and Biophysics, University of Iowa, Iowa City, Iowa 52242

MONTE WESTERFIELD
Department of Neurobiology, Harvard Medical School, Boston, Massachusetts 02115

ABSTRACT We have investigated the effects of postsynaptic membrane properties on the shape of synaptic potentials generated by time-varying synaptic conductances. We used numerical simulation techniques to model cells of several different geometrical forms, from an isopotential sphere to a neuron with a soma and a dendritic tree. A variety of postsynaptic membrane properties were tested: (*a*) a passive resistance-capacitance membrane, (*b*) a membrane represented by the Hodgkin and Huxley (HH) equations, and (*c*) a membrane that was passive except for a delayed rectification represented by a voltage- and time-dependent increase in G_K. In all cases we investigated the effects of these postsynaptic membrane properties on synaptic potentials produced by synaptic conductances that were fast or slow compared with the membrane time constant. In all cases the effects of postsynaptic rectification occurred on postsynaptic potentials of amplitudes as low as 1 mV. The HH model (compared with the passive model) produced an increased peak amplitude (from the increase in G_{Na}), but a decreased half-width and a decreased time integral (from the increase in G_K). These effects of the HH G_K change were duplicated by a simple analytical rectifier model.

INTRODUCTION

The membrane and cable properties of postsynaptic cells play important roles in determining the shape of postsynaptic potentials (PSP). Predictions of passive neuronal models have been compared to PSP recorded in motoneurons (Rall, 1962; Rall et al., 1967; Jack and Redman, 1971; Barrett and Crill, 1974) to determine how a cell's shape and the location of a synapse determine the efficacy of PSP. Similarly, the locations of synapses have been deduced from measurements of PSP shapes and the input resistance and transient response of postsynaptic cells (Rall et al., 1967; Jack et al., 1971; Iansek and Redman, 1973; Christensen and Teubl, 1979).

Nonlinear current-voltage relationships caused by changes in potassium conductance are a common feature of many excitable cells. Rectification in neurons was described over 40 years ago (Hodgkin, 1938), and the details of voltage-dependent potassium conductances are well characterized (Hodgkin and Huxley, 1952). The relative amount of rectification appears to vary considerably from cell to cell (Waltman, 1966; Hudspeth et al., 1977; Kleinhaus and Prichard, 1977; Adams et al., 1980). Recent experiments (Westerfield and Joyner, 1981) have shown that the potassium conductance of the squid axon reduces the efficacy of transmission at the giant synapse of the squid. Thus, it is of practical importance to determine the effects of postsynaptic membrane properties on the shape of PSP and to learn in what circumstances these effects may be important.

We report here the results of computer simulations of PSP generated in a neuronal model. By varying the membrane and cable properties of the model, we have been able to characterize how postsynaptic membrane conductances, both active and passive, influence the PSP shape. Our results demonstrate that observed amounts of postsynaptic rectification can dramatically reduce synaptic efficacy.

METHODS

Computer simulations were done to obtain the numerical solution for the PSP as a function of time for a model cell in response to a time-varying postsynaptic conductance (PSC). We used an analytical expression for the synaptic conductance (see Eq. 4). The electrical properties of the membrane of an isopotential cell (or a short length, Δx, of a nonisopotential cell) were represented by a resistance and capacitance in parallel, where a passive membrane was one in which the membrane resistance, R_m, remained constant. In simulations with active membrane responses, R_m was replaced by time- and voltage-dependent conductances (Hodgkin and Huxley, 1952) and is referred to as an HH membrane. The postsynaptic cell was modeled by (*a*) an isopotential membrane region, where

$$C\,dV/dt = -(I_s + I_m) \quad (1)$$

$$I_s = g_s(t)\,[V - E_R] \quad (2)$$

E_R = 70 mV (assumed reversal potential, relative to resting potential)
$I_m = V/R_m$ (for passive case) or

$$I_m = I_{HH} = I_{Na} + I_K + I_L \text{ (for HH case);} \quad (3)$$

Dr. Westerfield's present address is The Neuroscience Institute, Department of Biology, University of Oregon, Eugene, OR 97403.

(*b*) an integrative cell model, as described by Rall (1962), in which there were 21 compartments (1 for the soma and 20 for the dendritic tree).

The simulations were conducted using our previously published methods (Joyner et al., 1978) for modeling axons of varying radius. The relative values of the radii of the compartments were chosen such that the parameter ρ equals 4.0, where ρ is defined (Rall, 1959) as the ratio of the input conductance of the dendritic tree to the input conductance of the soma. Letting the Δx for our simulation be equal to 10% of the resting length constant of the dendritic cable makes the electrotonic length of the dendrites, L, equal to 2 (Barrett and Crill, 1974). The synaptic conductance was added to the membrane of one of these compartments. We treated the general case in which a PSP has an equilibrium potential 70 mV positive to the resting potential (Llinas et al., 1975) and let the synaptic conductance be represented, as a function of time, by

$$g_s(T) = \bar{g}_s e \alpha T e^{-\alpha T} \quad (4)$$

such that $g_s(T)$ will achieve its maximum value, $\bar{g}_s$, at $T = \alpha^{-1}$, where T is time in units of T_m, the resting membrane time constant. For the HH system, G_m at rest is 0.674 mS/cm^2, and T_m = 1.48 ms with C_m = 1 μF/cm^2. We thus compared the effects of synaptic conductances of varying time-course (by varying α) on an HH membrane and on a passive membrane with the same value of G_m. In addition, the HH membrane model was modeled at various temperatures by using a Q_{10} of 3.0 for all the HH rate constants. The charge entry produced by $g_s(t)$ was made independent of synapse location (for PSP amplitudes $\ll E_R$). From Eq. 4 it is clear that $\bar{g}_s$ is independent of α, and that the total charge entry ($\int g_s \, dt$) will be inversely proportional to α. The membrane properties of all compartments of the Rall model were assumed to be identical and were represented as patches of membrane (either passive or by HH equations [see above] or by a particular model of passive membrane combined with a simplified form of potassium rectification, Eq. 5). The simulations were performed in FORTRAN on a VAX 11/780 computer (Digital Equipment Corporation, Maynard, MA). Solutions for the cable model with HH membrane (21 compartments, Δt = 5 μs, total time 20 ms) required ~ 10 s of computation.

RESULTS

Response of HH Conductances to Small Voltage Changes

The response of the potassium conductance, G_K, is nonlinear near the resting potential. As shown in Fig. 1*A*, which plots the steady-state voltage dependence of the potassium conductance parameters, the n variable has a nearly linear relationship to voltage near the resting potential. G_K, however, shows a marked nonlinearity and changes nearly eightfold in the voltage range of ± 5 mV from the resting potential. We also computed the transient response of G_K to step changes in potential. Changes in G_K, in response to a rapid voltage change, occur with a time constant of about 4 ms at 6.3°C and ~0.6 ms at 26°C. As G_K comprises about half of the resting conductance, small changes in potential can produce significant changes in the input conductance of the cell. Therefore, small depolarizing synaptic potentials would be expected to alter G_K. Because the PSP depolarization is usually not long enough to produce steady-state changes in G_K, the effect would be smaller than for a maintained depolarization.

In the same voltage range, G_{Na} aso changes with potential (Fig. 1*B*). As the m and h parameters have different

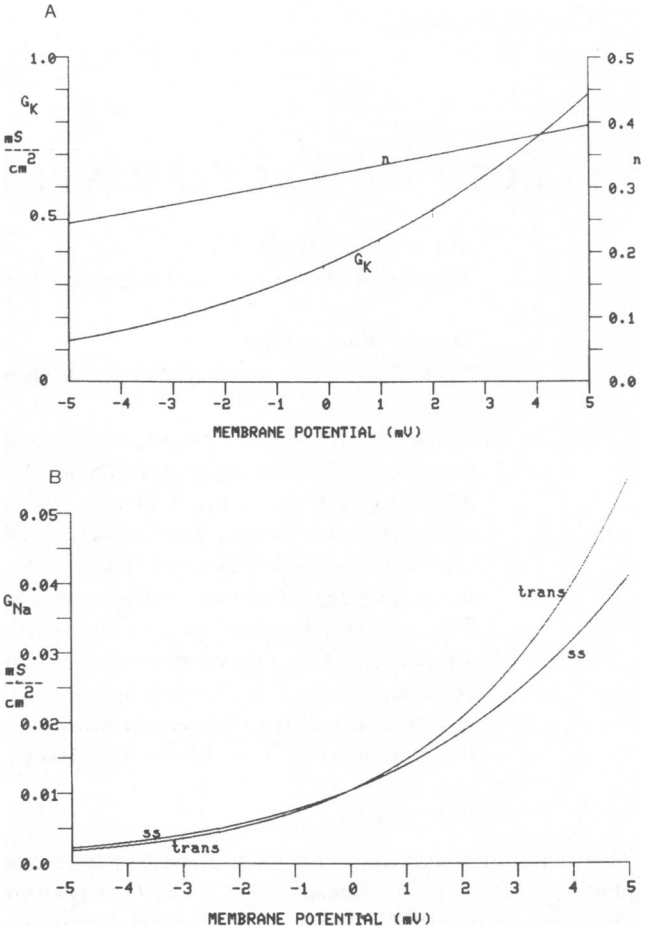

FIGURE 1 The voltage dependence of the HH conductances near the resting potential. In *A*, the voltage dependence of the HH potassium system is plotted near the resting potential. The steady-state values of n and G_K were calculated from the HH formulation and plotted as functions of membrane potential with respect to the resting potential (0 mV). In *B*, the voltage dependence of the HH sodium conductance (G_{Na}) near the resting potential is plotted. The steady-state (ss) and transient (trans) values of G_{Na} were calculated as functions of the membrane potential with respect to the resting potential (0 mV). The transient value was either the maximum value (for depolarizations) or the minimum value (for hyperpolarizations) obtained after a step change in potential.

time constants, there is (for depolarizing steps) a larger transient than steady-state increase in G_{Na} because m approaches its new higher value faster than h approaches its new lower value. Similarly, for a hyperpolarizing step, the transient decrease in G_{Na} is larger than the steady-state decrease. Even though the conductance changes for potassium are much larger than for sodium, the ~10-fold difference in their respective driving potential for current makes the G_{Na} changes significant in affecting the membrane potential response.

Response of Isopotential Membrane to Synaptic Conductances

Fig. 2 shows how the PSP shape in an isopotential passive membrane patch is affected by the time-course of the

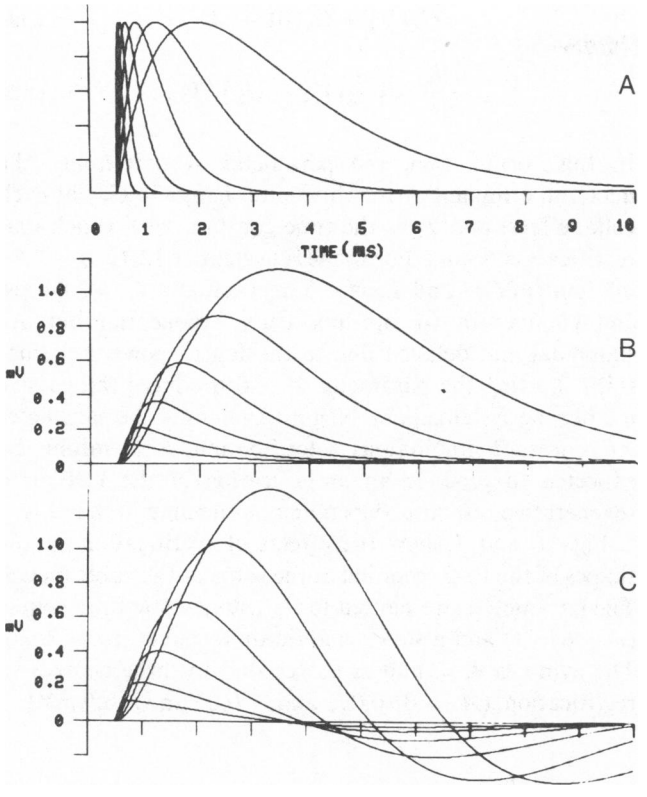

FIGURE 2 Effects of voltage-dependent postsynaptic conductances on PSP shape. PSP were simulated in response to synaptic conductance changes. In *A*, the synaptic conductances were calculated as functions of time from an analytical function with a series of α values (1,2,4,8,16,32) specifying progressively faster conductance changes. These synaptic conductances were inserted in parallel with two different postsynaptic membrane models to generate the PSP shown in *B* and *C*. In *B*, the PSP were calculated with a passive postsynaptic membrane model with a membrane resistance equal to the resting membrane resistance of the HH model. In *C*, the PSP were calculated using an isopotential patch of HH membrane.

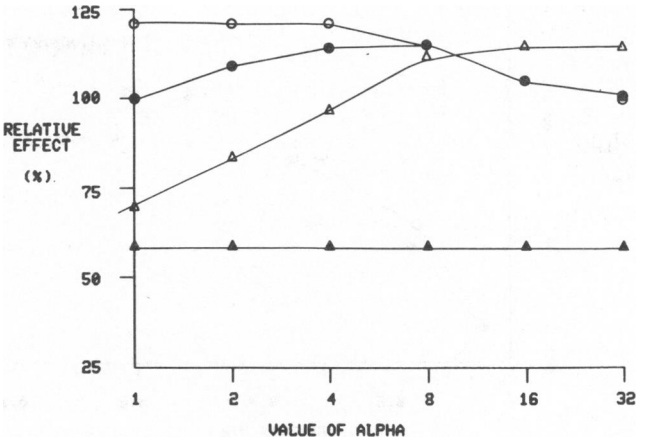

FIGURE 3 Relative effects of HH membrane properties on PSP shape parameters. Various parameters including maximum amplitude (○), rise time (●), half-width (△), and the time integral (▲), were computed from the PSP shown in Fig. 3 and were plotted as functions of the speed of the synaptic conductance (α). Each parameter is expressed as the active response (HH) relative to the passive response.

synaptic conductance and the postsynaptic membrane properties. As shown in Fig. 2*B*, the PSP rises and decays more slowly for smaller values of α (slower time-course of synaptic conductance). The amplitude of the PSP is small compared with E_R, because the magnitude of the synaptic conductance ($\bar{g}_s = 0.015$ mS/cm^2) is small compared with G_m; therefore, these results would be very similar to those obtained by injecting current with a time-course similar to $g_s(T)$. Fig. 2*C* shows the PSP for an HH membrane (12°C) for the same synaptic conductances shown in *A*. The voltage-dependent conductances have a dramatic effect on the PSP shape. There is an increase in the amplitude and rise time as well as changes in duration. These PSP also exhibit a marked hyperpolarization in response to all the synaptic conductances tested.

Fig. 3 shows the relative values of various parameters of the PSP shapes as functions of α, in a comparison of PSP generated by HH membranes at 12°C with those produced by a passive postsynaptic membrane. The PSP amplitude (○) is increased by active membrane properties, particularly for slower PSP (lower values of α). The rise time (●) also increases in an intermediate range of α values, but is not affected by active membrane properties for very fast or very slow PSP. The half-width (Δ) is shorter for slow PSP but longer for fast PSP. The time integral of the PSP (▲, taken over 20 ms) is decreased to 59% of the value for the passive membrane and the decrease is independent of the value of α.

Effects of Rectification on an Integrative Neuron Model

For the results presented so far, we have assumed that the postsynaptic region is part of an isopotential cell. To study the effects of the cable properties of the postsynaptic cell of the PSP shape, we simulated the response of a neuron with a soma and a dendritic tree. Synaptic conductance (varying with time) was placed at a synaptic location, X, representing the distance (in units of the resting length constant) from the soma, and we evaluated the shape of the PSP generated at the soma. Fig. 4 shows (for fast [*A*] and slow [*B*] PSC time-courses) the relationships between rise time and half-width of the PSP recorded at the soma of a cell with passive properties (●) or HH properties (○). Each solid line connects a series of results (from left to right) in which X was varied from 0 to 2 in steps of 0.5. For the fast PSP ($\alpha = 64$), there is little effect of voltage-dependent postsynaptic conductances unless X is >1.0. For the slow PSP ($\alpha = 2$), the presence of HH membrane produces a decrease in half-width for a given rise time at all synaptic locations, with the effect being most dramatic at higher values of X.

As shown for the isopotential case (Fig. 3), the time integral of the PSP is also considerably reduced by the presence of voltage-dependent postsynaptic membrane

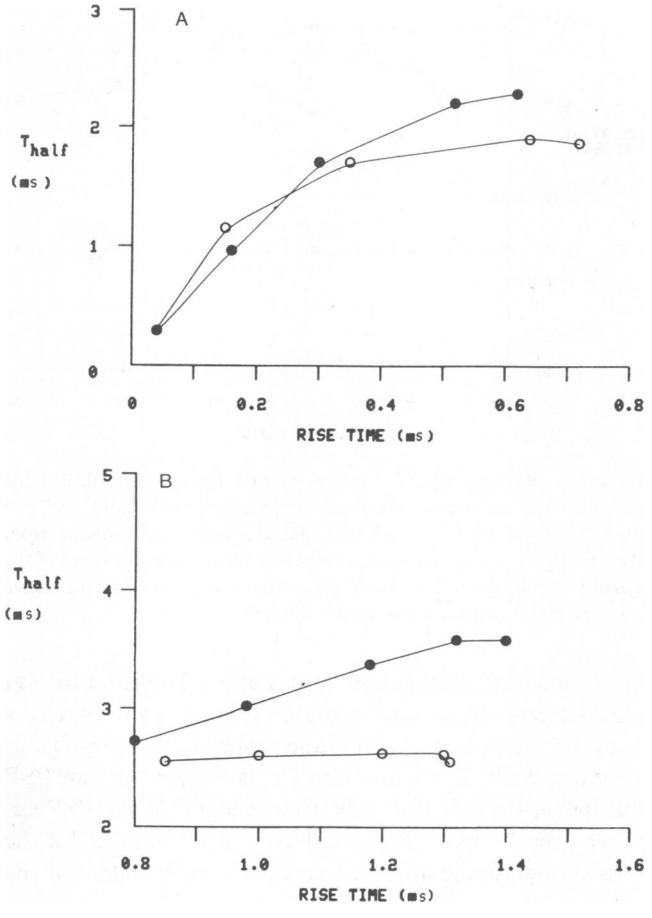

FIGURE 4 Effect of synaptic location on PSP shapes. Shape parameters of simulated PSP measured at $X = 0$ were calculated for synapses located at varying distances (X) from the soma compartment of a neuron represented by a Rall model with $\rho = 4$, $L = 2$. Two different synaptic time-courses were used: fast ($\alpha = 64$) in A, and slow ($\alpha = 2$) in B. In each case, the effect of X on the half-width and rise time was determined for active (HH equations at 12°C) (○) and passive (●) (resistance equaled resting resistance of HH equations) membrane models. Each solid line connects a series of results (left to right) in which X was varied from 0 to 2 in steps of 0.5.

conductances in this cable model of the neuron, Fig. 5 shows the integral response of cells with HH or passive membrane to fast (A) and slow (B) PSC, as a function of X. The reduction due to the HH properties varies from 30% (for a somatic synapse) to 63%, for a synapse at $X = 2$. On the logarithmic scale, it is clear that the percent reduction of this integral is independent of the time-course of the synaptic conductance (comparing A with B), but is increased by increasing X, the electrotonic distance from the soma to the synaptic site.

To consider the mechanism by which the PSP shapes are affected by active postsynaptic membrane properties, we eliminated voltage-dependent conductances except for G_K and replaced the HH equations by a simpler analytical form. Thus, we reduced the HH system to the following: $G_m = G_L + G_K$ where $E_L = +10$ mV, $E_K = -10$ mV, and, at rest, $G_K = G_L = 0.337$ mS/cm^2. For the rectification of G_K, we let G_K vary with voltage and time as

$$\bar{G}_K(V) = \bar{G}_K(0) + AV \tag{5a}$$

$$\frac{dG_K}{dt} = [\bar{G}_K(V) - G_K]/T_K. \tag{5b}$$

In this formulation, the parameter A determines the maximum amount of rectification (change in G_K) at each voltage level and T_K is the time constant with which that rectification occurs. For the HH system at 12°C, $A = 0.07$ mS/cm^2(mV)$^{-1}$ and T_K is ~ 5 ms (actually $T_n = 2.84$ ms, and changes in G_K are not truly exponential but are sigmoidal and delayed due to the fourth power relationship). Letting the parameter $A = 0$ produces the passive membrane system again. Negative values of the parameter A represent anomalous rectification and might be expected to produce an amplification of the PSP or a regenerative response, depending on the magnitude of A.

Figs. 6 and 7 show the effects of rectification on the shapes of the PSP recorded at the soma of the cable model. The parameters are plotted for a fast synaptic time-course ($\alpha = 64$, A) and a slow synaptic time-course ($\alpha = 2$, B). The symbols ●, ○, and △ correspond to three degrees of rectification ($A = 0$, 0.07, and -0.02 mS/cm^2(mV),$^{-1}$

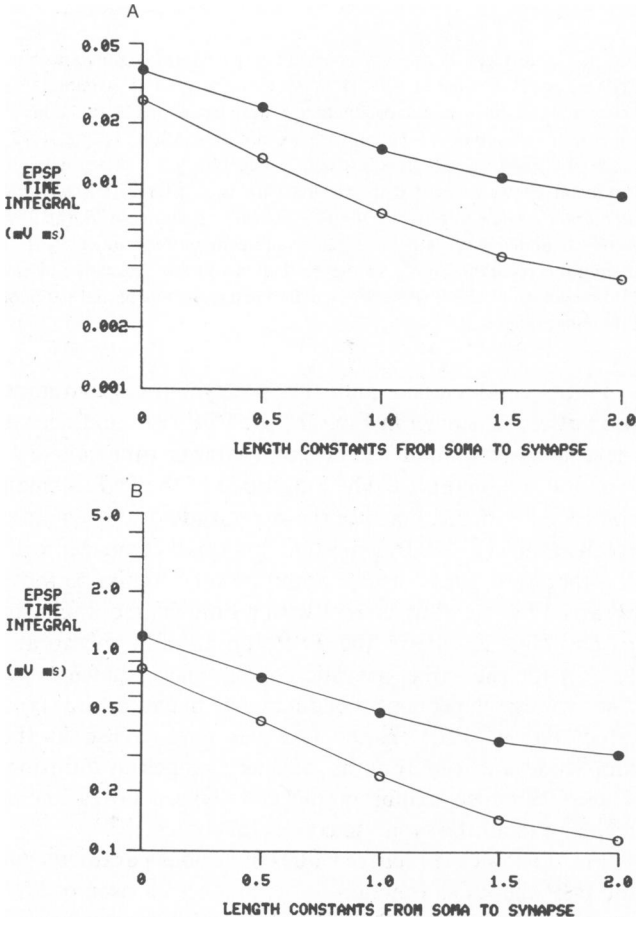

FIGURE 5 Effects of synaptic location on the time integral of the PSP. Time integrals were calculated from PSP simuated as in Fig. 4. ●, passive; ○, HH 12°; $\alpha = 64$.

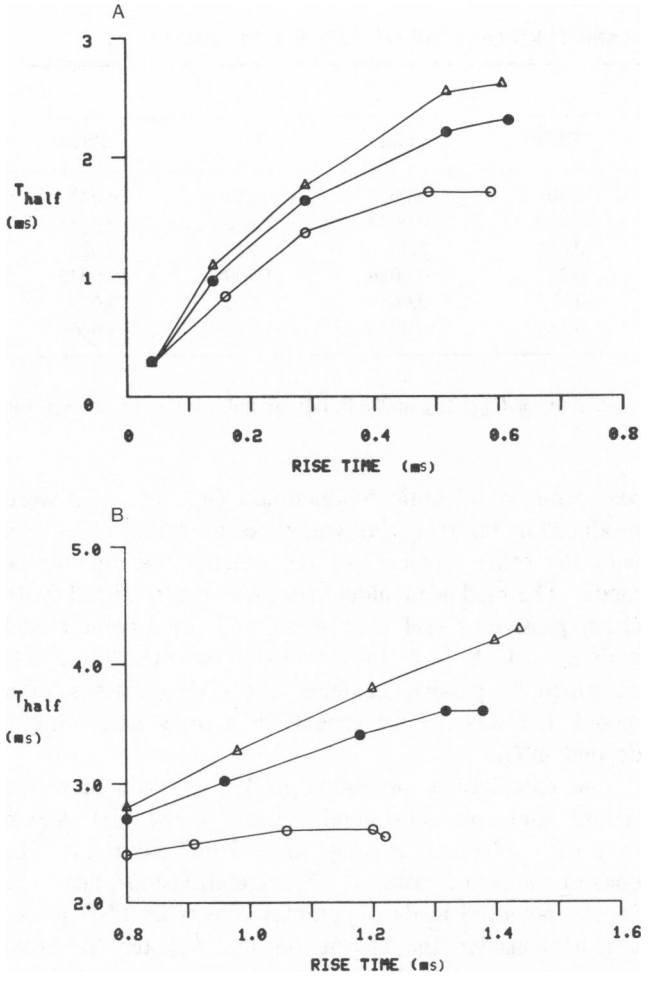

FIGURE 6 Effects of rectification on PSP shapes. PSP were simulated with a simplified form of the HH membrane model containing only potassium and leakage conductance. Potassium conductance was calculated with an analytical expression (Eq. 5) in which the parameter A, representing the amount of potassium rectification, determined the potential dependence of the slope of the conductance change. PSP were calculated as in Fig. 4. For △, $A = -0.02$; for ●, $A = 0$; for ○, $A = 0.07$. In A, $\alpha = 64$; B, $\alpha = 2$.

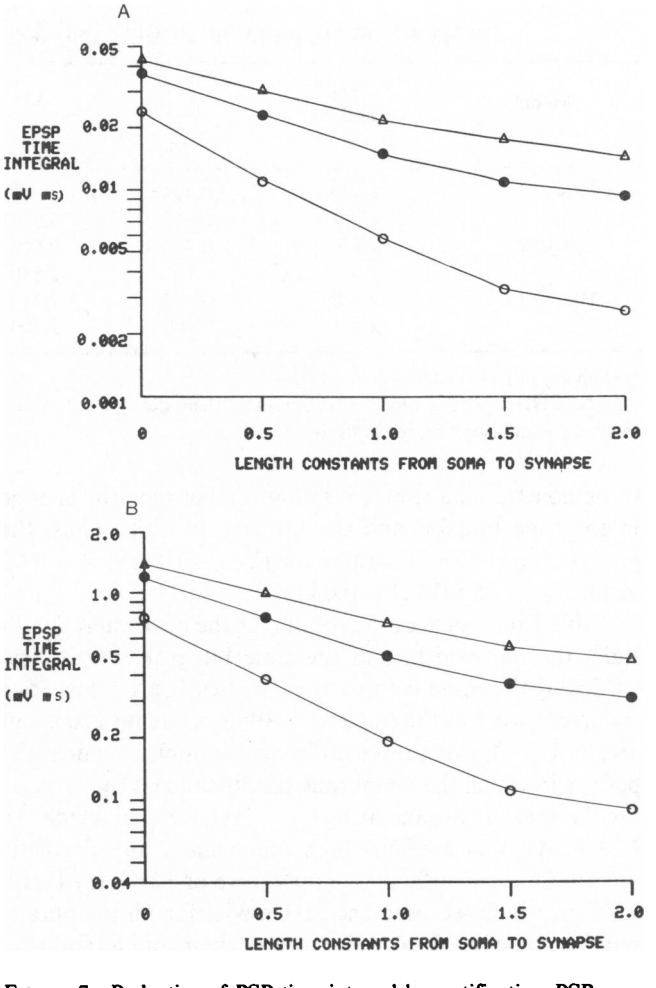

FIGURE 7 Reduction of PSP time integral by rectification. PSP were simulated as in Fig. 6. △, $A = -0.02$; ●, $A = 0$; 0, $A = 0.07$. For A, $\alpha = 64$; for B, $\alpha = 2$.

respectively). Fig. 6 shows that the relationship between half-width and rise time is dramatically changed by rectification. As in Fig. 4, each solid line connects a series of results (from left to right) in which X was varied from 0 to 2 in steps of 0.5. The reduced HH formulation for rectification produces a decrease in half-width and shows that this effect is particularly apparent for the slower PSC time-course. For an even slower PSC time-course ($\alpha = 0.5$, not shown), the relationship is so distorted for $A = 0.07$ that the slope is negative, indicating that, for somatic recording, a distal dendritic PSP would have a shorter half-width than a somatic PSP with the same synaptic conductance time-course.

Fig. 7 shows how the amount of rectification changes the relationships between the time integral of the PSP and the synaptic location. Using the same symbols as in Fig. 6, the data for $\alpha = 64$ and $\alpha = 2$ are plotted logarithmically against X. As was shown for the HH model (Fig. 5) the decrease in PSP integral, indicating the decrease in effective charge transfer to the soma, varies with the synaptic location but is independent of the time-course of the PSC.

These effects are not simply due to a change in the membrane conductance. Examining a particular case ($\alpha = 64$, $X = 1$, $A = 0$), the PSP amplitude was 56 μV at the synaptic site and 7.2 μV at the soma. When rectification was included ($A = 0.07$) the corresponding values of PSP amplitude were unchanged yet the rectification produced a two and a half times decrease in the time integral of the PSP recorded at the soma (from 0.015 to 0.006 mV · ms). When these same simulations were run with the membrane model changed so that the values of G_K and G_L were the same but both E_K and E_L were set to zero, the PSP amplitudes at the synaptic site and somatic site were the same as before, but now the same amount of rectification ($A = 0.07$) produced no change in the time integral of the PSP recorded at the soma (PSP time integral = 0.0151 for $\alpha = 64$, $X = 1$, $A = 0$; PSP time integral = 0.0151 for $\alpha = 64$, $X = 1$, $A = 0.07$). Substituting various values for E_K and E_L (always keeping $E_K = -E_L$ and $G_K = G_L$ at $V =$

TABLE I
EFFECTS OF MEMBRANE MODEL AND α ON PARAMETERS OF EPSP RECORDED AT SOMA*

Model type	Synaptic location (λ)	$\alpha = 2$			$\alpha = 64$		
		V_{max}	$T_{1/2}$	$\int$ PSPdt	V_{max}	$T_{1/2}$	$\int$ PSPdt
Passive	$x = 0$	0.396	2,700	1.203	0.06	280	0.037
	$x = 1$	0.123	3,360	0.490	0.0073	1,650	0.0151
HH 12°C	$x = 0$	0.440	2,510	0.852	0.06	320	0.026
	$x = 1$	0.165	2,650	0.243	0.0086	1,700	0.0075
HHN‡ 12°C	$x = 0$	0.375	2,210	0.715	0.06	280	0.023
	$x = 1$	0.109	2,290	0.165	0.0070	1,190	0.0063

*Geometry in Rall model with $\rho = 4$, $L = 2$.
‡HHN is HH model in which m and h retain their steady-state values for $V = 0$. Units of V_{max}, $T_{1/2}$, and $\int$ PSPdt are millivolts, microseconds, and millivolts × milliseconds, respectively.

0) demonstrated a simple relationship between the change in the time integral and the product $A \cdot E_K$. Thus, the effects on PSP were the same for $E_K = -10$ mV, $A = 0.02$ as for $E_K = -5$ mV, $A = 0.04$.

Table I summarizes the results for the maximum amplitude, the half-width, and the time integral of PSP (recorded at the soma compartment) when fast or slow PSC occurred either at the soma ($X = 0$) or one length constant away ($X = 1$), using three different membrane models: (*a*) passive in which the membrane conductance is the same as for the HH membrane at rest. (*b*) HH 12°C in which the HH model was used for both the somatic and dendritic membrane at an effective temperature of 12°C. (*c*) HHN 12°C in which we used the HH model for all membrane but did not allow the kinetic parameters m and h (and thus G_{Na}) to change with time from their steady-state values for $V = 0$.

During the slower PSC, where $\alpha = 2$, active membrane conductances (HH 12°C) increased the PSP amplitude 11% above the passive response, while the model with only g_K rectification (HHN 12°C) decreased it 5%. Both alterations decreased the half-width and time integral of the PSP, and all of these effects were more prominent for a dendritic synapse ($X = 1$) than for a somatic synapse ($X = 0$). For the faster synaptic conductance ($\alpha = 64$), neither the HH 12°C nor the HHN 12°C model produced significant changes in the maximum amplitude or half-width of the PSP for a somatic synapse, although both decreased the time integral of the PSP. However, for a dendritic location ($X = 1$), the effects of membrane rectification were similar to those observed at somatic locations with slower synaptic conductances. It is clear that large effects on the PSP time integral are produced by changes in the potassium conductance.

DISCUSSION

We have presented here an examination of how the electrical properties of the post synaptic cell affect the shape of the PSP. We used an analytical function to scale the synaptic conductance [$g_s(T)$, Eq. 4] for a slow ($\alpha = 2$) or fast ($\alpha = 64$) time-course, while maintaining a constant peak value of synaptic conductance, ($\bar{g}_s$). The PSP were produced by inserting the synaptic conductance in parallel with the other elements of the postsynaptic membrane model. The models included: (*a*) an isopotential cell (with either passive or HH membrane, and (*b*) a cable model with $\rho = 4$, $L = 2$. In the model the membrane was described by passive elements, the HH equations, or a model that was passive except for a time- and voltage-dependent G_K.

The calculations presented in Fig. 1 show how the sodium and potassium conductances of the HH system vary with voltage in a range of ± 5 mV from rest. The nonzero slope of both of these relationships near the resting potential leads to complex effects on PSP shape. Let us consider the effects on the isopotential patch (summarized in Fig. 3). Because G_{Na} increases with depolarization, all depolarizing PSP will increase I_{Na} above its resting level. As this change occurs very rapidly, there will be a tendency to increase the PSP amplitude, as compared with the response produced by a passive membrane with the same resting conductance. Depolarizing PSP will also activate G_K. The delayed rise in G_K, however, tends to decrease the width of the PSP and produce an after hyperpolarization. The width is considerably decreased by this mechanism for slow PSP (low α). For fast PSP, the width is increased by G_{Na}, because G_K does not have time to activate. One of the most interesting features of this dual rectification is that, with the HH model, the time integral of the PSP decreases (to 59% of the value for a passive membrane) independently of the value of α chosen for $g_S(T)$ (Fig. 3). This decrease in time integral occurs even in cases where both the maximum amplitude and the half-width are increased (e.g., $\alpha = 8$).

Several points are illustrated by the simulations using the Rall cable model for a neuron (Figs. 4–7). For the passive membrane model, the PSP shape depends on the cable properties ρ, L, G_m, membrane capacitance), the location of the synaptic input, and the time-course of the synaptic conductance (see Jack et al., 1975). In our simulations we first compared the results for the passive membrane with those obtained when the membrane was

described by the HH model (Figs. 4 and 5). Effects on PSP shape (as recorded at the soma) were similar to those obtained for the isopotential patch, with the additional feature that these effects were even greater for synapses occurring on the dendritic region than for synapses occurring on the soma. The time integral of the PSP was especially affected, being much less for synapses located at a greater electrotonic distance from the soma. By comparing results with and without voltage-dependent sodium conductances (Table I), we show that the amplitude increases were due to changes in G_{Na} whereas the decreases in the time integral were due to changes in G_K.

Simplifying the description of potassium rectification (Figs. 6–7) illustrated the mechanism by which rectification affects the PSP shape and time integral. The relationship between rectification and PSP shape can be demonstrated analytically in the following way.

For an isopotential cell $-C\,dV/dt = I_s + G_L(V - E_L) + G_K(V - E_K)$, integrating with respect to time yields $0 = \int I_S dt + (G_L + G_K) \int V dt$ because $\int dV/dt\,dt = 0$, and $G_L E_L = -G_K E_K$, because the net current in the resting state must be zero.

Then, the time integral of the PSP is $\int V dt = -\int I_s dt/(G_L + G_K) = (Q/G_L + G_K)$, where Q is the charge that enters the cell due to the synaptic conductance. However, if $G_K = \bar{G}_K(0) + AV$ (assuming T_K is vanishingly small) then $-C\,dV/dt = I_S + G_L(V - E_L) + [\bar{G}_K(0) + AV)](V - E_K) = I_S + [G_L + \bar{G}_K(0)]V + AV^2 - AVE_K$, because $G_L E_K = -\bar{G}_K(0)E_K$. Assuming that the PSP amplitude is always $\ll |E_K|$, then the term AV_2 is small and can be neglected, leaving $\int V dt = -\int I_S\,dt/[G_L + \bar{G}_K(0) - AE_K]$.

The ratio of the time integral of V with $A \neq 0$ to the time integral of V with $A = 0$ is $[G_L + \bar{G}_K(0)]/[G_L + \bar{G}_K(0) - AE_K]$. Thus, because E_K is negative, there is a decrease in the time integral of the PSP that depends on the product AE_K as shown by the results. For the values of A and E_K that approximate the HH potassium rectification, this equation predicts a reduction of the PSP time integral to 44.5% of the value obtained with a passive membrane. Simulation of an isopotential membrane patch with either passive membrane or this rectifier model produced the following results: for a PSP generated by a conductance function with $\alpha = 2$, $\bar{g}_s = 0.00002$ S/cm^2, the PSP integral was 4.14 mV · ms for the passive membrane and 1.822 for the rectifier membrane, giving a ratio of 0.44. This result was quite insensitive to the value of T_K, varying < 1% for $0 < T_K < 10$ ms. Recent experiments with the squid giant synapse (Westerfield and Joyner, 1981) have demonstrated that the voltage-dependent potassium conductance produces an after hyperpolarization and a decreased half-width of PSP only a few millivolts in amplitude. Thus, normal amounts of potassium rectification can dramatically reduce the charge transferred to a cell by synaptic activity.

The effects of rectification due to a voltage-dependent increase in potassium current are fundamentally different from the effects produced by an inhibitory PSC that acts by increasing the total membrane conductance. As illustrated analytically and in the results presented with the simplified G_K model, the PSP integral is reduced by charge leaving the cell as an induced potassium current and not by the conductance increase, per se. In the example shown in Fig. 7*A* ($X = 1$), the presence of rectification reduced the PSP integral two and a half times, even though the maximum PSP amplitude was only 0.056 mV and the maximum change in G_K was < 0.004 mS/cm^2 (< 2% of its resting value). By contrast, a steady conductance added in parallel to the passive model, as at inhibitory synapses, would have to be three times as large as the resting potassium conductance to produce the same decrease in PSP time integral. This distinction also helps explain why there is a constant percentage decrease of the PSP time integral in our results (for a given cable model and membrane model) when we vary the PSC time-course (and thus the PSP amplitude) over a 32-fold range.

For the cable model, potassium rectification reduces the PSP integral more for dendritic than for somatic synaptic locations (see Fig. 7). For a somatic synapse, a large part of the charge enters as I_S goes into the dendrites. Thus the somatic PSP amplitude (and threfore the amount of rectification) is less for a given amount of charge entry than in an isopotential cell. For a dendritic synapse, the PSP recorded at the soma is affected not only by rectification at the synaptic site, but also by rectification (and progressive charge loss) through the membrane between the synaptic site and the soma. Thus, for dendritic synapses, the time integral of the PSP recorded at the soma is decreased more by a given amount of rectification than in an isopotential cell.

The results suggest that rectification, due to potassium conductance increase, produces a dramatic decrease in the time integral of the PSP. Thus, the efficacy of synapses is greatly reduced by this form of rectification. Furthermore, this reduction is much greater at distally located synapses than at synapses located on the cell's soma.

This work was supported by National Institutes of Health grants NS15350 to Dr. Joyner and NS03437 and NS11613 to Dr. J. W. Moore.

Received for publication 2 August 1981 and in revised form 20 October 1981.

REFERENCES

Adams, D. J., S. J. Smith, and S. H. Thompson. 1980. Ionic currents in molluscan soma. *Annu. Rev. Neurosci.* 13:141–167.

Barrett, J. N., and W. E. Crill. 1974. Influence of dendritic location and membrane properties on the effectiveness of synapses on cat motoneurones. *J. Physiol. (Lond.).* 293:325-345.

Christensen, B. N., and W. D. Teubl. 1979. Localization of synaptic input on dendrites of a lamprey spinal cord neurone from physiological measurements of membrane properties. *J. Physiol. (Lond.).* 297:319-333.

Hodgkin, A. L. 1938. The subthreshold potentials in a crustacean nerve fibre. *J. Physiol. (Lond.).* 126:87–121.

Hodgkin, A. L., and A. F. Huxley. 1952. A quantitative description of membrane current and its application to conduction and excitation in nerve. *J. Physiol. (Lond.).* 117:500–544.

Hudspeth, A. J., M. M. Poo, and H. E. Stuart. 1977. Passive signal propagation and membrane properties in median photoreceptors of the giant barnacle. *J. Physiol. (Lond.).* 272:25–43.

Iansek, R., and S. J. Redman. 1973. An analysis of the cable properties of spinal motoneurones using a brief intracellular current pulse. *J. Physiol. (Lond.).* 334:613–636.

Jack, J. J. B., S. Miller, R. Porter, and S. J. Redman. 1971. The time course of minimal excitatory post-synaptic potentials evoked in spinal motoneurones by group Ia afferent fibres. *J. Physiol. (Lond.).* 215:353-380.

Jack, J. J. B., and S. J. Redman. 1971. An electrical description of the motoneurone, and its application to the analysis of synaptic potentials. *J. Physiol. (Lond.).* 215:321–352.

Joyner, R. W., M. Westerfield, J. W. Moore, and N. Stockbridge. 1978. A numerical method to model excitable cells. *Biophys. J.* 22:155-170.

Kleinhaus, A. L., and J. W. Pritchard. 1977. Close relation between TEA responses and Ca-dependent membrane phenomenon of four identified leech neurones. *J. Physiol. (Lond.).* 270:181–194.

Llinás, R., R. W. Joyner, and C. Nicholson. 1974. Equilibrium potential for the postsynaptic response in the squid giant synapse. *J. Gen. Physiol.* 64:519–537.

Rall, W. 1959. Branching dendrite trees and motoneuron resistivity. *Exp. Neurol.* 1:491–527.

Rall, W. 1962. Theory of physiological properties of dendrites. *Ann. N.Y. Acad. Sci.* 96:1071–1092.

Rall, W., R. E. Burke, T. G. Smith, P. G. Nelson, and K. Frank. 1967. Dendritic location of synapses and possible mechanisms for the monosynaptic EPSP in motoneurons. *J. Neurophysiol.* 30:1169–1153.

Waltman, B. 1966. Electrical properties and fine structure of the ampullary canals of Lorenzini. *Acta Physiol. Scand. Suppl.* 264:1–60.

Westerfield, M., and R. W. Joyner. 1982. Postsynaptic factors controlling the shape of potentials at the squid giant synapse. *Neuroscience.* In press.